Towards single photon microscopy

THESIS

submitted in partial fulfillment of the
requirements for the degree of

MASTER OF SCIENCE
in
PHYSICS

Author :	A.W.E. van Vark
Student ID :	.....
Supervisor :	Dr. W. Löffler
2^{nd} corrector :	Prof. dr. ir. T.H. Oosterkamp

Leiden, The Netherlands, July 8, 2019

Towards single photon microscopy

A.W.E. van Vark

Huygens-Kamerlingh Onnes Laboratory, Leiden University
P.O. Box 9500, 2300 RA Leiden, The Netherlands

July 8, 2019

Abstract

In this thesis I explore the possibility of excitation with a single photon source for biomicroscopy purposes. In biomicroscopy the fluorescent properties of molecules are used to label proteins or molecules of interest. A key limitation is the effect of photobleaching: after some time all fluorescent molecules are irreversibly converted to a dark state. Photobleaching processes involve highly reactive excited states of molecules and formation of radical oxygen. Excitation with single photons represses multiphoton processes and it is therefore expected that this will reduce the photobleaching rate. So far no experiments have been done with bright cavity based single photon sources. If the cavity based single photon source at our disposal is integrated in the microscopy setup, this could be a first test system for single photon microscopy.

Contents

Chapter 1

Introduction

In biomicroscopy images are taken of living cells or tissue. This is done using fluorescence. Fluorescent emitters can be divided in two types, the intrinsic fluorophores that occur naturally and the extrinsic fluorophores that can be added to a sample to obtain the desired spectral properties. Examples of extrinsic fluorophores are molecules, fluorescent dyes or quantum dots. A very special class of fluorophores are the fluorescent indicators, whose spectral properties change when bound to another substance. These fluorophores can for instance be used to determine the abundance of the substance they are bound to.

Fluorescence microscopy allows the detection of single molecules and tracking of proteïns or molecules of interest, which can be labeled with a fluorescent marker. Going one step further, the emission spectrum of the markers can yield additional information on the properties of the complexes they are bound to.

The key issue in using fluorescence to perform either microscopy or spectroscopy is the effect of photobleaching: after some time the fluorophores undergo an irriversible transition to a dark state and stop emitting altogether. The timescale on which bleaching occurs can range from seconds to hours, depending on the sample, temperature and excitation intensity.

It is known that the single-photon character of the emission can be exploited, for example in superresolution microscopy. Two simultaneously registered photons indicate the presence of multiple single photon emitters. By measuring higher order correlations, images with a higher resolution than the diffraction limit can be created. This raises the question whether excitation with single photons can be exploited as well.

Over the last two decades single photon sources have been developed

that can deterministically produce a stream of photons with fluctuations below the shot noise limit. Therefore they are of great interest for applications such as quantum imaging and enhanced precision measurements. Recently the single photon sources have also become very bright, producing single photon streams with a rate of up to around 22 MHz [1], which could in principle be as high as 1 GHz without much modification.

In this thesis I will explore the possibility of using single photons for biomicrosopy purposes and if this could reduce photobleaching. First of all, in chapter 2 I will discuss the processes involved in photoluminescense both on the molecular level as well as for bulk materials and quantum dots after which I consider possible photobleaching pathways. I present the microscopy setup built to perform spectroscopy and show the photoluminescence spectrum of GaAs. The quantum character of light is discussed in chapter 3, starting with the statistics of a light beam. Then I will go into detail about the generation of squeezed and entangled states and most importantly single photon streams. In chapter 4 I will review the current state of the art of using quantum light for spectroscopy. Finally, in the last chapter I provide a summary and conclusion.

Chapter 2

Photoluminescence

2.1 Molecular fluorescence spectroscopy

Fluorescence vs. phosphorescence
Photoluminescence (PL) is the emission of light from matter following absorption of photons. The mechanism behind this emission is photoexcitation, where an electron is excited to a higher electronic state. For single emitters, photoluminescence can be divided in two categories. If the excited state is a singlet state (S_1), the electron in the excited orbital has the same spin as a second electron in the ground state. Therefore the transition to the ground state (S_0) is dipole allowed and occurs rapidly (typical rate near 10^8 s^{-1}). This radiative emission is called fluorescence. Another pathway exists in the case that the excited electron undergoes spin conversion and ends up in a triplet state (T_1). After this intersystem crossing, the transition to the ground state is dipole forbidden. As a consequence the excited state has a much larger lifetime (typically $10^{-3} - 1$ s), which gives rise to the phenomenon called blinking: a dead time where the emitter does not emit. Emission from this transition is called phosphorescence. The lifetimes can even be much longer which becomes apparent in glow in the dark substances.

Processes involved in the PL scheme are generally illustrated by Jablonski diagrams. Figure 2.1 shows a simplified diagram of fluorescence and phosphorescence of a molecule. The structure of the energy levels of molecules, consisting of electronic, rotational and vibrational states, lead to characteristic absorption and emission spectra. A molecular PL spectrum has a few characteristic features, which will be discussed in the following paragraph.

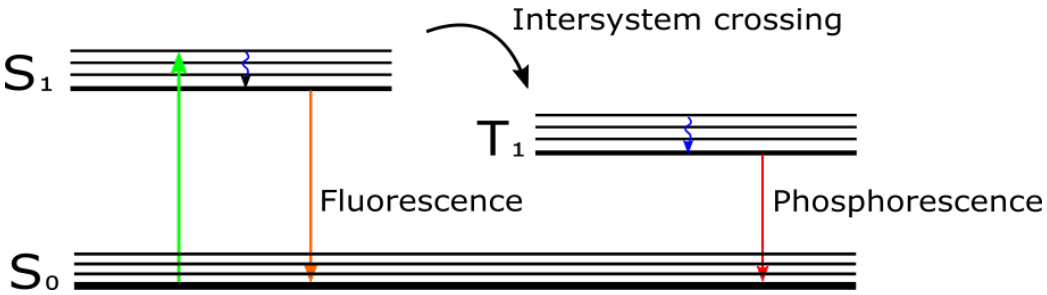

Figure 2.1: *Simplified Jablonski diagram illustrating the difference between fluorescence and phosphorescence. The blue arrows indicate nonradiative internal conversion.*

Stokes shift and the mirror-image rule

The Stokes shift is the difference in wavelength of the absorption and emission peaks of the same electronic transition. For most molecules the absorption shifts to higher wavelengths. The emission peak shifts to higher wavelengths when an excited electron loses energy, due to vibrational relaxation or dissipation and solvent reorganisation, before returning to the ground state. Transitions between vibrational states occur on a timescale much faster than transitions between electronic states. Therefore we can say that all electronic transitions happen from a vibrational ground state, as was already illustrated in figure 2.1. While the emission spectrum of most molecules is shifted to higher wavelengths, the opposite can also happen. If the excited electron gains energy from dissipation of thermal phonons the emission peak shifts to lower wavelengths, which is called an anti-Stokes shift.

Electronic transitions are vertical, that is, they occur without change in the position of the nucleus. This statement is called the Franck-Condon principle. Quantum mechanically formulated, a transition is more likely to occur if the wave functions of the involved vibrational levels have more overlap. As a result, if a transmission is most likely to happen in absorption, its reciprocal transition is most likely to happen in emission [2]. It should be noted that this approximation only holds in the condensed phase and for rigid molecules. The same argumentation of overlapping wave functions explains that molecules emit in appreciable yield only from the first excited singlet state, see figure 2.2. This is known as Kasha's rule.

Combining these three factors, it follows that the emission spectrum of a molecule is the mirrored image of the S_0-S_1 transition. This is visu-

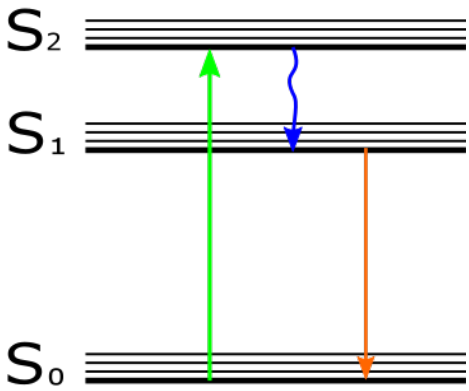

Figure 2.2: *Simplified Jablonski diagram illustrating Kasha's rule. Although excitation to the second excited level is possible, the emission is only from the first excited state.*

alised in figure 2.3. Since only one state yields emission, an equivalent of Kasha's rule is that the shape of the emission spectrum is independent of the excitation wavelength. Exceptions to this rule arise when there are large energy gaps between excited states.

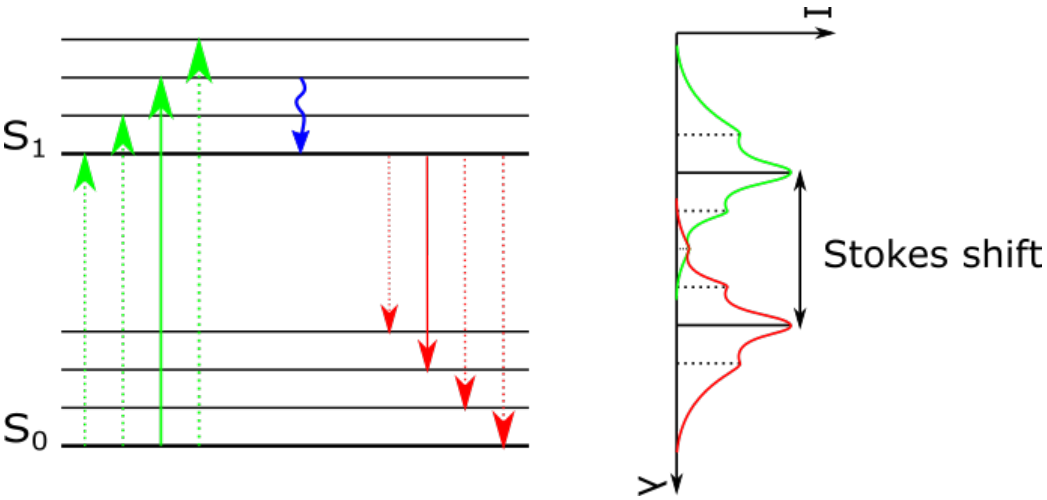

Figure 2.3: *Implementation of the Franck-Condon principle and Kasha's rule illustrated to explain the mirrored spectra. The blue arrow indicates non-radiative internal conversion.*

Quantum yield and fluorescent lifetime
A fluorophore is not fully characterized by the Stokes shift alone. An important property is its quantum yield: the ratio between the number of emitted and absorbed photons. Substances with a large quantum yield have bright emissions. Another property of interest is the lifetime of a fluorophore, which depicts the time available for interaction with its environment. Its importance will become clear in the section on photobleaching reactions.

Fluorescence quenching and anisotropy
For some applications a high intensity PL spectrum is required. However, this is not necessarily obtained by a higher concentration of fluorophores. Sometimes adding more fluorophores can even have the opposite effect. The decrease in intensity of fluorescence is called quenching. We can distinguish collisional and static quenching. The excited state fluorophore can be deactivated by making contact with another molecule and returning non-radiatically to the ground state or the fluorophores can form non-fluorescent complexes. Quenching also occurs due to the attenuation of incident light by self-shielding or other absorbing species.

Another factor that can limit the intensity of the fluorescence is the photoselective absorption of polarized light. Light is preferentially absorbed or emitted by matter if the electric vector is parallel to the absorption transition dipole. As a result, when excited with polarized light, the fluorescence emission is also partially polarized. The photoselectivity of fluorophores can be exploited in anisotropy measurements, which can be used to provide information on the shape and size of proteins or to investigate the rigidity of molecular environments.

More detailed information can be found in the "IUPAC. Compendium of Chemical Terminology" [3] and in the first chapter of "Principles of fluorescence spectroscopy" by Lakowicz [4]

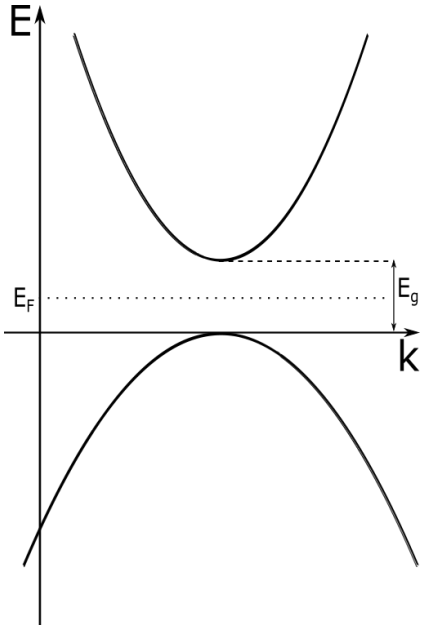

Figure 2.4: *Example of a band diagram of a perfect direct-gap semiconductor. The Fermi engergy (E_F) lies in the middle of the bandgap (E_g).*

2.2 Photoluminescence spectrum of a semiconductor

Band structure
So far only single emitters have been considered. While for ensemble measurements the discussed processes hold they do not apply to bulk materials. The discrete nature of the vibrational bands disappears in a bulk material and the electronic states form a band structure where we can no longer distinguish between fluorescence and phosphorescence. In a semiconductor material the valence and conduction bands are separated by a band gap. For direct-gap semiconductors the bottom of the conduction band and the top of the valence band can be approximated as parabola, as is shown in figure 2.4.

The PL process in a semiconductor material is similar to that in a molecule. A PL spectrum of a semiconductor can be taken when exciting with a laser that emits photons with an energy higher than the bandgap energy (E_g). Upon photoabsorption, electrons are excited to the conduction band, leaving holes in the valence band. Then, through scattering interactions and interactions with phonons, the electrons relax to the bottom of the conduc-

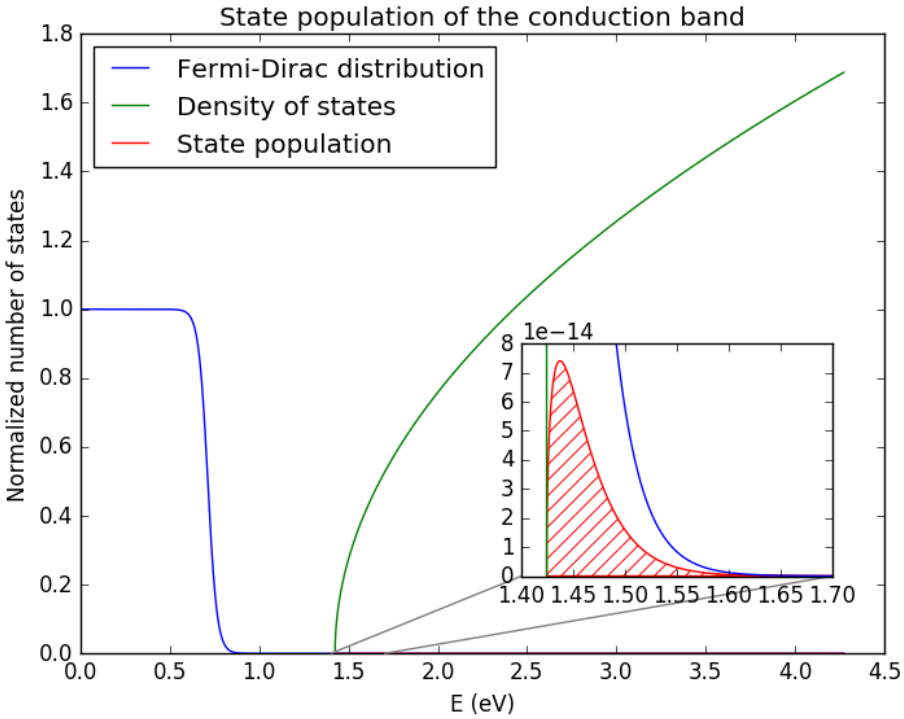

Figure 2.5: *Illustration of the population of the conduction band for a perfect GaAs semiconductor at room temperature (T = 300 K). The Fermi level lies in the middle of the bandgap of E_g = 1.42 eV. The marked area in the inset shows the population of the conduction band.*

tion band before recombining radiatively with a hole. The PL spectrum thus reflects the density of holes in the valence band.

The theoretical PL spectrum can be calculated quite easily for a direct bandgap non-degenerate semiconductor such as GaAs. The density of states for electrons in a 3D system scales with the square root of the energy:

$$DOS(E) \sim \sqrt{E - E_g}. \tag{2.1}$$

In thermal equilibrium the Fermi-Dirac distribution describes the electron occupation probability as a function of energy:

$$f(E) = \left(e^{(E-E_F)/k_BT} + 1\right)^{-1}. \tag{2.2}$$

Here k_B is the Boltzmann constant and E_F is the total chemical potential or Fermi-level. In metals, the Fermi-level lies inside one of the bands, whereas in semiconductors and insulators it lies inside the band gap. However, in semiconductors the conduction band is close enough to be thermally populated. The population of the states is given by the product of the Fermi-Dirac distribution and the density of states as function of energy. Following the same argumentation, we find the same shape for the population of holes. The PL spectrum thus takes the form of the overlap integral shown in the inset of figure 2.5.

GaAs spectrum

As part of this project I built a microscopy setup to explore the issues and efficiencies working towards a setup suitable to perform single photon microscopy. One step in this process was to take a PL spectrum of GaAs.

The microscopy setup is shown in figure 2.6. The sample is mounted on a movable stage and is illuminated with a 632.8 nm HeNe laser that is coupled to the setup via a single mode optical fiber. The laser beam is collimated using a microscope objective (10x, NA = 0.25) and has an incoming power of approximately 1 mW which can be changed using an attenuation filter. Using the Spiricon620U CCD camera for alignment, the laser beam is focused on the sample by a second microscope objective (20x, NA = 0.4). The PL emission is measured in reflection and is sent to the spectrometer via a beam splitter. A longpass filter (> 700) filter is placed in the optical path to separate the emission from reflected laser light. A third microscope objective (10x, NA = 0.25) couples the light into a multimode fiber, connecting the microscopy setup to the Triax 550 spectrometer that is equipped with an Andor Idus CCD (DU 401A-BR-DD). The PL spectra were taken with a 600 lines/mm grating with a blaze of 1000 nm. The wavelength of the spectrometer had to be manually calibrated using the position of the 632.8 nm peak.

In fig 2.7 the PL spectra of GaAs taken at different incoming powers are shown. All spectra have an integration time of 1.5 s and were normalized, after background subtraction, in order to compare the shapes.

The resulting spectra differ somewhat in shape as compared to the theoretical prediction. A clear deviation from fig 2.5 is the appearance of a tail at the low energy side as opposed to the predicted sharp cut-off. That the cut-off is not sharp can be explained by the fact that the theoretical spectrum was that of a perfect semiconductor. In reality a sample has defects that create a tail in the band edge.

Furthermore, GaAs has a bandgap of 1.42 eV [5], but in the obtained

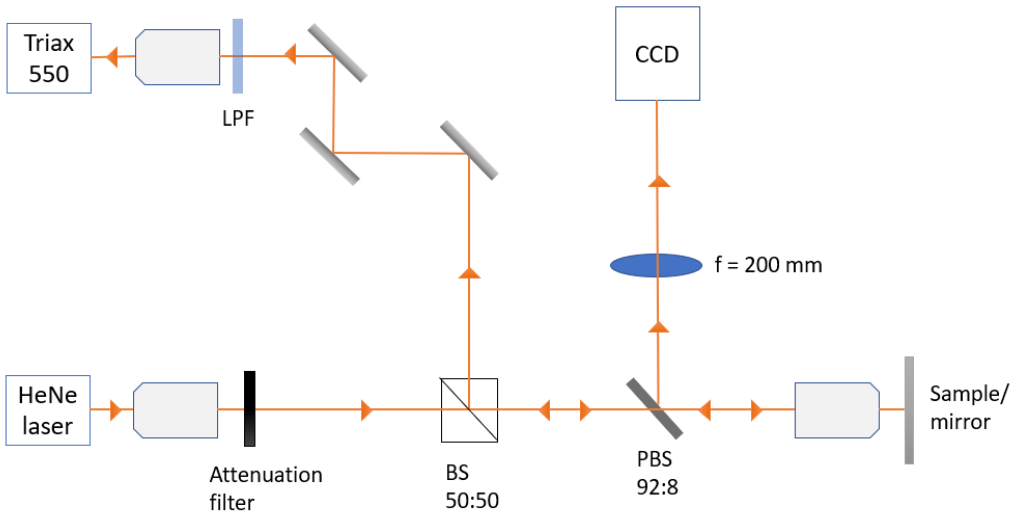

Figure 2.6: *Setup used to take the GaAs spectrum. The sample is mounted on a movable stage and is illuminated by a 632.8 nm HeNe laser with variable incoming power. The beam is focused in the sample using a microscope objective (20x, NA = 0.4) and is aligned using an image on a Spiricon620U CCD camera. The emitted light is send to the spectrometer by a beam splitter (BS) and is separated from reflected laser light by a longpass filter (LPF) > 700 nm. The laser and Triax 550 spectrometer are fiber coupled to the setup using microscope objectives (10x, NA = 0.25).*

spectra the bandgap lies below this value and appears to shift to lower energies for higher intensities. The shift could be partly due to an error in calibration (99% linearity). The intensity dependence on the low energy side can be due to a phenomenon called bandgap renormalization. The width of the bandgap decreases monotonically as function of the electron-hole-pair density. If the electrons and holes were distributed randomly in the sample, the Coulomb forces would cancel and the bandgap would be independent of this density. However, Pauli's exclusion principle forbids parallel spins in the same unit cell, so on average the distance between the fermions is greater. This reduces the Coulomb repulsion, thus lowering the total energy of the system [6].

Looking at the peaks of the spectra, they seem to broaden and shift to higher energies. This could be explained by a temperature increase scaling with intensity that increases the Fermi energy and broadens the Fermi-Dirac distribution.

Finally, on the high energy side of the spectra there is a feature that increases with increasing energy. This could be due to phase space filling.

Carriers fill the band from the bottom. When the concentration increases, the number of high energy carriers increases. As a result the optical gain increases for shorter wavelengths [7].

There are many complex processes involved in the photoluminescence of a semiconductor that each lead to characteristic features in the spectrum. It is therefore extremely difficult to find out what exactly causes the observed shapes and this goes beyond the scope of this project.

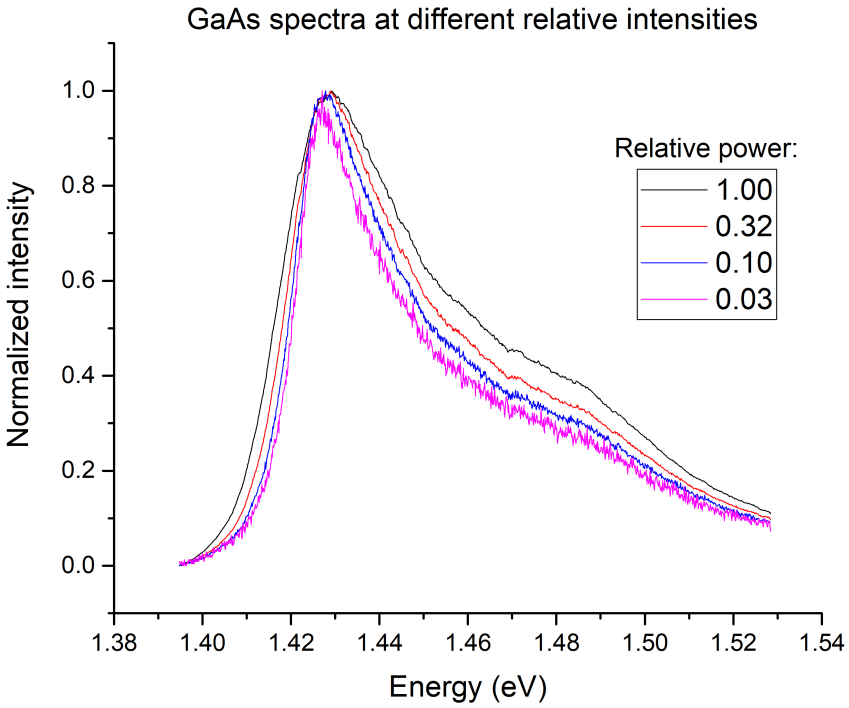

Figure 2.7: *Photoluminescence spectra of a GaAs semiconductor at room temperature (T = 300K) excited with a 632.8nm HeNe laser. The laser beam was attenuated to obtain spectra for different intensities. After background subtraction the spectra were normalised in order to compare their shapes.*

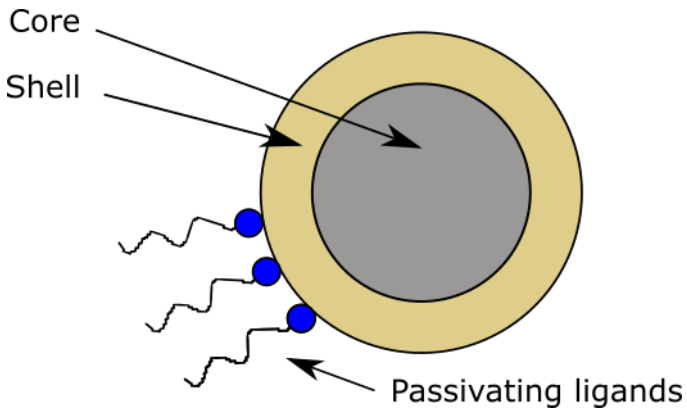

Figure 2.8: *Schematic of a core-shell quantum dot.*

2.3 Quantum dots as fluorescent markers

Quantum dots are fluorescent semiconducting nanocrystals, the radius of which is comparable to the materials Bohr exciton radius [8]. An exciton is created when a weak attractive Coulomb force exists between an excited electron in the conduction band and the hole in the valence band of a semiconductor. The medium quantum confinement in three directions leads to discrete energy levels for both the hole and the electron analogous to the particle in the box problem. The bandgap is dependent on the size of the crystal, thus the radius of the quantum dot provides a way to tune the emission [9]. The quantum confinement is manifested by encapsulating the crystal with organic surfactants. These bonds however form non-radiative relaxation pathways and lower the fluorescent quantum yield of the crystals. To counter this issue the crystals can be coated with another semiconducting material. Such a configuration, which is called a core-shell quantum dot, has the further advantage that surface defects as dangling bonds, that can create non-radiative sites, are reduced [10]. A schematic of a core-shell quantum dot is shown in figure 2.8.

Core shell quantum dots have different properties as compared to fluorescent dyes and conventional molecular fluorophores [11]. The emission of quantum dots is generally narrower than that of molecules. Conventional dyes have small Stokes shift and narrow absorption and emission spectra. Working with different dyes for color labeling is therefore often complicated because the dyes need to be excited at a specific wavelength. Quantum dots on the other hand have a very broad absorption spectrum and can be excited at any wavelength below their characteristic absorbtion

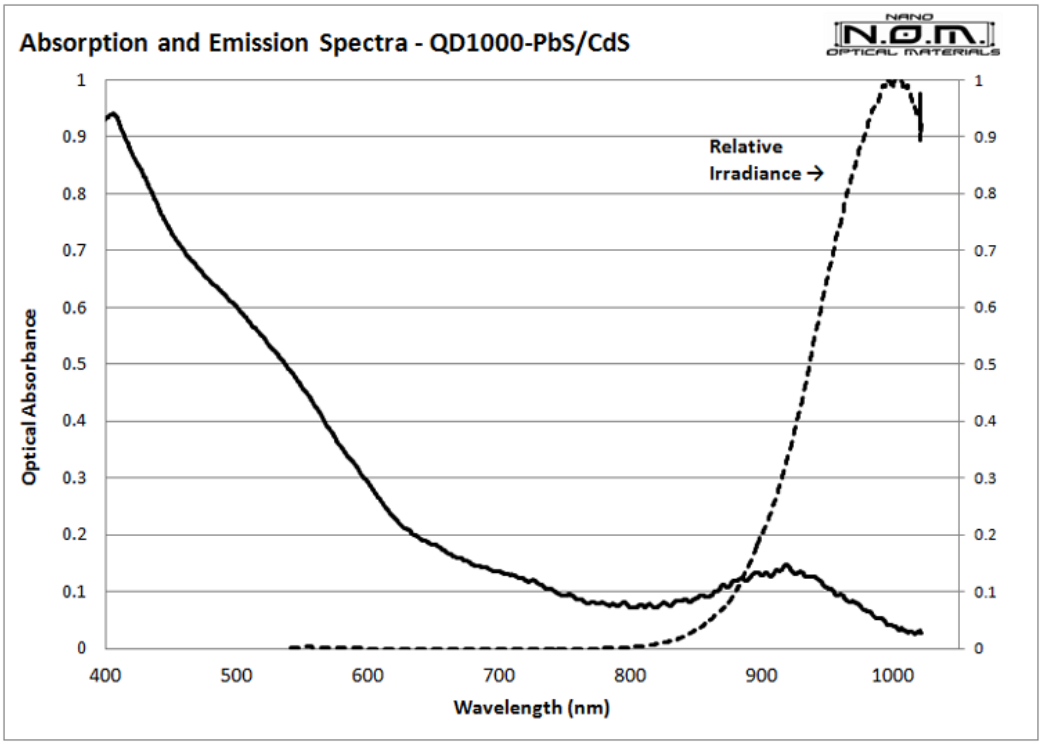

Figure 2.9: *Absorption and emission spectrum of PbS/CdS Near infrared Quantum Dots with a peak emission of 1000nm. The characteristic absorption (first exciton peak) lies around 930 nm, but the qantum dots can be excited at shorter wavelengths as well.*

wavelength, as can be seen in figure 2.9. This property can be explained by the fact that the probability of creating an electron-hole pair by absorption of a photon above the semiconductor bandgap increases with energy. The lifetime of an exciton is typically much longer than that of fluorophores. Another advantage is that quantum dots have a high resistance to photobleaching. Quantum dots have been reported to maintain stability up to a few hours while organic fluorophores typically bleach after only a few minutes of exposure [12].

Quantum dots are particularly useful in near infrared (NIR) spectroscopy, as most conventional fluorophores emit in the visual range. Because of the longer wavelength, NIR radiation is less prone to scattering effects and can penetrate deeper into a sample. On the other hand there are concerns regarding the toxicity of quantum dots when used for in vivo labeling. Primary issues are the presence of heavy metal ions and phototoxicity due the generation of reactive oxygen [13].

2.4 Photobleaching

Blinking and bleaching in fluorescent molecules
Photobleaching is the irreversible conversion of a fluorescent molecule to a non-fluorescent state. This is in contrast with the dark states associated with blinking that are temporary. It is well known that blinking occurs when intersystem crossing transforms the dye molecule to the long-lived triplet state, or when the molecules becomes negatively charged and a radical anion state is formed. On the other hand, the exact mechanism of photobleaching is not yet fully understood, although several theories have been proposed to explain this phenomenon. The main cause seems to involve photodynamic interaction with molecular oxygen, which is one of the few molecules which has a triplet ground state. The relatively long lifetime of the triplet excited state of the dye molecule allows interactions with triplet oxygen that generate singlet oxygen. Singlet oxygen has an even longer lifetime and when it decays, several types of damaging oxygen free radicals can be created. Furthermore, a dye molecule in a triplet or anion state is highly reactive and can undergo irreversible chemical reactions with nearby organic molecules [14]. Secondary photobleaching occurs when the dark triplet and anion states are optically excited. The photobleaching rate is dependent on the lifetime of the lowest triplet and anion states and on the intensity of the excitation [15]. A Jablonski diagram describing possible blinking and bleaching pathways is shown in figure 2.10.

Blinking and bleaching in quantum dots
Blinking and photobleaching also occur in colloidal quantum dots. However, the phenomena can not be explained in the same way as for molecular dyes as quantum dots do not have an excited triplet state. Blinking of a quantum dot, referred to as PL intermittency, was discovered in 1996 by single-molecule spectroscopy of a single colloidal QD [16]. To account for the blinking, the report suggested an ionization-deionization scheme involving the formation of trions. A trion state is a three carrier state that is created when a charge carrier, an electron or a hole, is lost via surface defects previous to absorption of another photon. The trions trigger Auger processes that act as non-radiative decay channels, quenching the fluorescence. After deionization the QD goes back to its fluorescence cycle [17]. Bleaching of the quantum dots, also referred to as photodarkening, could be due to decomposition by photo-oxidation reactions [18].

The effects of PL intermittency and photobleaching can be suppressed by chemically passivating the surface defects and dangling bonds by coat-

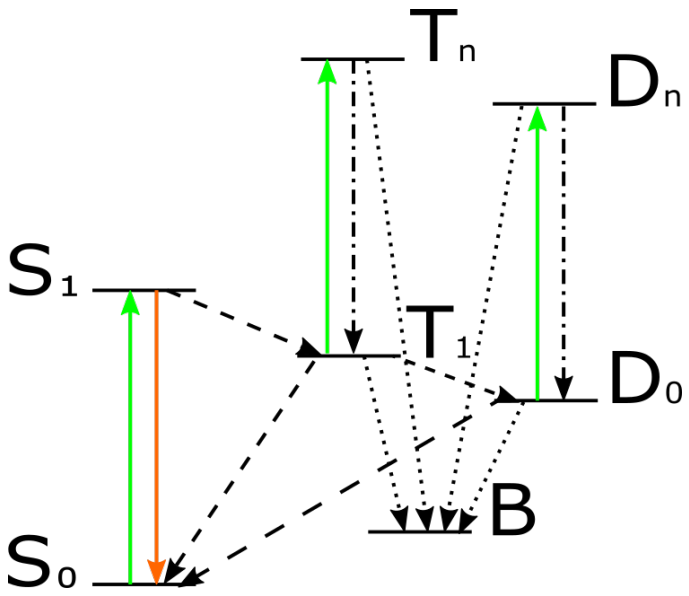

Figure 2.10: *Jablonski diagram illustrating possible photoblinking and -bleaching pathways of a molecule indicated by dashed and dotted arrows respectively. The singlet electronic ground (S_0) and first excited state (S_1) are included in the figure as well as the lowest triplet (T_1) and anion (D_0) states, and their excited states (T_n, D_n) and lastly the bleached state (B). Solid arrows indicate radiative transitions and internal conversion is indicated by the dashed-dotted arrows. Figure adapted from [15].*

ing the QD's with a shell consisting of large bandgap semiconductor material or organic polymers. Using these techniques quantum dots have been developed that are photostable for hours. Even fluorescent nanodiamonds that show no photobleaching have been reported, which have the additional advantage that they also tackle the problem of phototoxicity in biological samples [19]. However, these nanodiamonds are not tunable and emit in the visual range.

Photobleaching does not always have to be a limiting factor. It can be exploited to measure the kinetic effects of diffusion as is done in fluorescence revovery after photobleaching (FRAP) measurements. This is done by photobleaching a tiny volume and measuring the fluorescence over time. By diffusion the dark molecules in the bleached region will be replaced by molecules that still exhibit fluorescence.

Chapter 3

Quantum light

3.1 Quantum nature of light

Classically light is described as an oscillation electromagnetic field. In the quantummechanical picture, where energy is quantized, light is described as a quantization of this field and can be thought of as particles travelling with the speed of light, which we call photons.

Statistics
The closest analogy to a classical state is a perfectly coherent monochromatic light beam with constant intensity, such as (to good approximation) laser light. Looking at the photon statistics, this light has a Poissonian number distribution

$$P(n) = \frac{\bar{n}^n}{n! e^{\bar{n}}}, \tag{3.1}$$

where the probability to find n photons depends only on the average number of photons $\bar{n}$. The fluctuations of the light are described by the variance, which in the Poissonian case corresponds to $(\Delta n)^2 = \bar{n}$. In conventional imaging this is the shot noise limit (SNL) where the signal to noise ratio is equal to $\frac{\bar{n}}{\sqrt{\bar{n}}} = \sqrt{\bar{n}}$.

According to the variance, light can be classified into three types: Poissonian, super- and sub-Poissonian. Classically there is no state with a lower variance than a coherent state and any light beam with varying intensity will have super-Poissonian statistics. It follows that sub-Poissonian light has no classical counterpart and has to be described fully quantummechanically. The purest sub-Poissonian light is the photon number state,

also called Fock state, which has zero variance. Any other state of light can be described in the basis of Fock states.

Losses and the ultimate quantum limit
Sub-Poissonian light, though fairly easy to generate in a laboratory, is difficult to observe. In particular, optical losses in the detection path form a serious issue. Losses are best modeled by visualizing a lossy medium as a perfect beam splitter with transmission probability T and the vacuum at the second input. The effect of loss is thus equivalent to random sampling of the photons. If a light beam with a mean photon number $\bar{n}$ impinges on such a beam splitter, the chance of m out of n photons being transmitted is given by the binomial distribution, which has a variance of T(1-T)$\bar{n}$. The variance of the photon stream then changes accordingly:

$$(\Delta n')^2 = T^2(\Delta n)^2 + T(1-T)\bar{n}. \tag{3.2}$$

For low values of T, we see that $(\Delta n')^2 \approx T\bar{n}$. Thus randomization of the photon stream degrades the statistics to the Poissonian case. This sets a fundamental lower limit, called the ultimate quantum limit (UQL) on the variance. The degradation to the shot noise limit is shown in figure 3.1.

Losses occur when using inefficient collection optics, when optical components scatter, reflect or absorb light and when detectors have insufficient quantum efficiency. In order to observe large quantum effects, high efficient detectors are needed and optical losses must be avoided.

Only one very special type of squeezed light does not alter under these losses, namely the single photon Fock state. One of the exceptional properties of this state is that whenever losses occur, there will still be single photons interacting with the sample.

A more complete explanation on photon statistics can be found in chapter 5 of "Quantum Optics: An Introduction" by Fox [21].

3.2 Quantum states of light

The interest in quantum light for spectroscopy is twofold, namely exceptionally low noise and strong correlations [22]. In this convention the term quantum light refers to light that exhibits sub-Poissonian statistics, in particular squeezed and entangled states.

Version of July 8, 2019– Created July 8, 2019 - 19:27

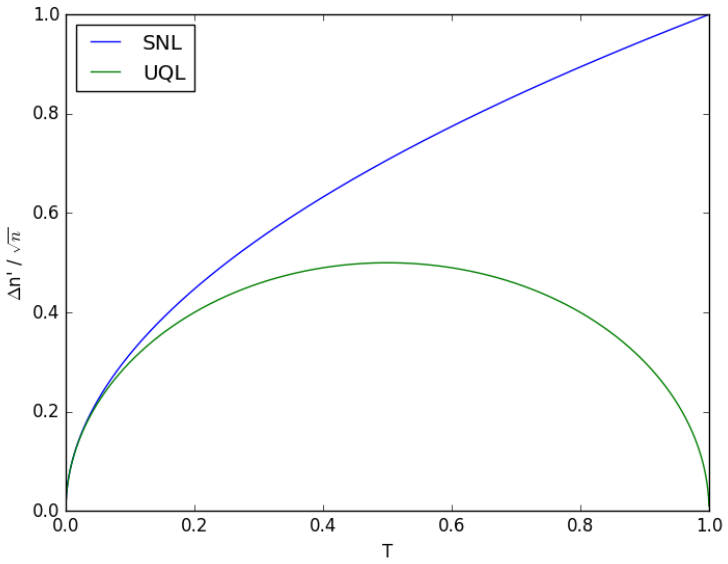

Figure 3.1: *The uncertainty in photon number, $\Delta n'$, as function of the transmission T for Poissonian light, the shot noise limit (SNL), and a Fock state, the ultimate quantum limit (UQL). Figure adapted from [20].*

Coherent and squeezed states

In analogy with the quantum harmonic oscillator, the quantized electromagnetic field is subject to the Heisenberg uncertainty principle:

$$\Delta x \Delta p \geq \frac{\hbar}{2}. \tag{3.3}$$

In terms of field quadratures (X_1, X_2), field amplitudes that can be directly related to generalized position and momentum coordinates, this uncertainty is manifested when

$$\Delta X_1 \Delta X_2 \geq \frac{1}{4}. \tag{3.4}$$

The aforementioned coherent states are balanced minimal uncertainty states where $\Delta X_1 = \Delta X_2 = \frac{1}{2}$. The quantum fluctuations of the vacuum state inhibit this uncertainty. Any state for which one of the quadratures falls below this limit is called squeezed. As a consequence of the Heisenberg principle, it follows that the conjugate quadrature must show larger fluctuations, see figure 3.2.

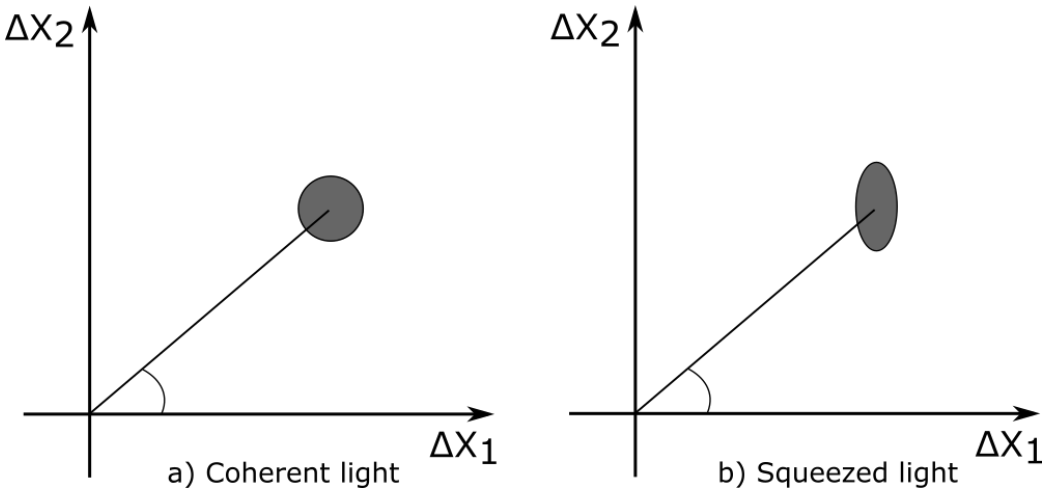

Figure 3.2: *Quadrature squeezing illustrated.*

The squeezed part of the light can be accessed by measuring the field quadratures. This can be achieved by using a relatively simple interference technique known as balanced homodyne detection. The setup involves a strong local oscillator and measurement of the intensity difference. A simple mathematical description is given in the squeezed light paper by Lvovsky [23]. Figure 3.3 shows the photon number distribution for a squeezed vacuum state where only even photon number states occur.

Entangled light
Two photons are entangled if the state of one can not be described independently of the state of the other. Light can become entangled in different ways. The most common degrees of freedom that become entangled are position and momentum, energy, spin and polarization. Measurement on one photon then yields information on the state of the other. Entangled photon pairs can be created in various ways including decay of doubly excited states in semiconductors, four-wave mixing or parametric downconversion (PDC) [24]. From here on we focus on the latter, as it is also a source of single photons and squeezed light.

Parametric downconversion
A PDC setup, see figure 3.4, consists of strong pump laser parametrically driving a nonlinear medium that has a non-vanishing second order susceptibility ($\chi^{(2)}$), for example a birefringent crystal. Inside the medium, the pump photons are converted into photon pairs, called a signal and an idler. The photons of such a pair are assumed to be created instanta-

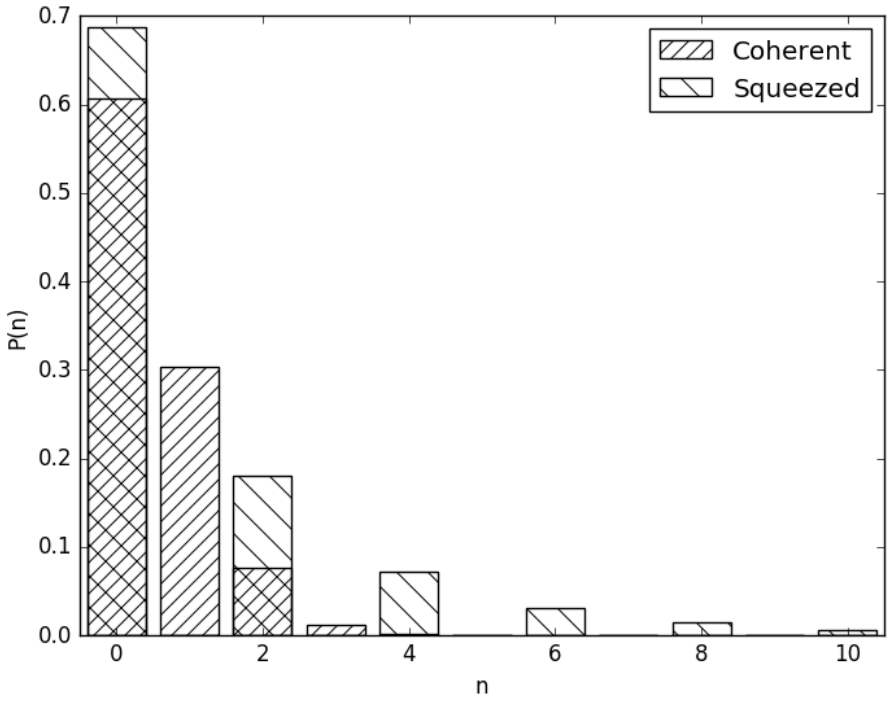

Figure 3.3: *Histogram of the photon number distribution of a coherent and a squeezed vacuum. In the latter case only even photon numbers occur.*

neously [25]. Due to conservation of energy and momentum, also referred to as the phase-matching condition, they show high time and frequency correlations. The photon pairs created in a PDC process are thus entangled in frequency, position and momentum [26]. The process is probabilistic instead of deterministic, but, because the photons are created in pairs, the measurement of one photon can be used to herald the other. This makes PDC also a heralded single photon source.

One can distinguish type I and II downconversion dependent on the relative polarizations of the pump, signal and idler beams.

In type I downconversion, the signal and idler beams have the same polarization that is orthogonal to that of the pump. The pair is emitted at the opposite sides of two concentric cones. Degenerate type I PDC, where both photons leave the crystal along the same axis and are indistinguishable, provides a way to generate single mode squeezed light, leading to a distribution as in figure 3.3. The downside of using a PDC process is that

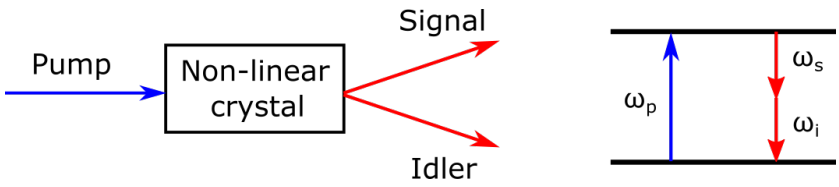

Figure 3.4: *PDC setup. A pump beam is converted by a nonlinear crystal to a signal and an idler beam which are entangled in frequency, position and momentum.*

the rate at which photon pairs are produced is relatively low (efficiency $\approx$ 10^{-7} - 10^{-11} [27]). To enhance the obtained squeezing the pump intensity needs to be increased, for example by using an ultrashort pulsed laser or by placing the crystal in a Fabry-Perot cavity [28]. This last configuration is called an optical parametric amplifier or oscillator.

In type II downconversion, the signal and idler beams have orthogonal polarizations. Due to birefringence effects the photons are emitted at the opposite sides of two intersecting cones. The intersections are of particular interest because they are sources of polarization entangled light.

Two photon-absorption microscopy

An application of entangled light in the field of biomicroscopy is two-photon absorption. This microscopy technique uses two photons of half the excitation wavelength to excite a molecule to a higher electronic energy state. The excitation is a single absorption event, which means that the photons must hit the sample within a femtosecond. This requires a high power and fast pulsed laser with a tight focus. The technique has several benefits. The excitation is restricted to a tiny focal volume, so that by scanning a 2D or even 3D image of the sample can be obtained and the overall photobleaching and phototoxicity is reduced. Furthermore, the longer excitation wavelength penetrates deeper into the sample and scatters less. Additionally, because only one photon is emitted when the molecule returns to the ground state, the fluorescence is easily separable from the excitation light.

Classically the intensity of two-photon fluorescence scales quadratically with the intensity of the excitation beam. At low intensities when two consecutive photons are entangled, this relation is linear [29]. The deviation to quadratic scaling at higher intensities can be explained statistically by the high photon density that reduces the chance that two photons are from the same pair. The linear scaling of such classical heterodyne signals by use of entangled light, allows the use of much lower photon fluxes for

microscopy and lithography applications.

3.3 Single photons

Purity and indistinguishability
The ideal single photon source produces indistinguishable single photons on demand [27]. The single photon character, or purity, can be charactized by a second order correlation measurement. This can be done using a Hanbury-Brown and Twiss interferometer which measures coincidences between counts on two single photon detectors. The second order correlation function can be written in terms of photon numbers as

$$g^{(2)}(\tau) = \frac{\langle n_1(t) n_2(t+\tau)\rangle}{\langle n_1(t)\rangle \langle n_2(t+\tau)\rangle}, \tag{3.5}$$

where $n_i(t)$ is the number of photons that detector i measures at time t. A perfect single photon stream has a $g^{(2)}(0)$ of 0.

The indistinguishability of photons in a photon stream can be checked via the Hong-Ou-mandel effect. If two photons are indistinguishable, their paths will interfere. When these photons arrive at separate inputs of a beam splitter, they will both leave from the same output, causing a dip in a coincindence measurement. Indistinguishability is of particular importance in quantum information experiments. However, if we want to employ single photons for microscopy or spectroscopy purposes, their indistinguishability is not relevant. We need a source that is bright and has a high purity.

Single photon sources
Until recently, PDC generated heralded single photon sources were the state of the art [30]. However, their use is limited because there is always a trade-off between the purity and the brightness of the source due to the probabilistic nature of the pair production. For a deterministic generation of single photons at a high rate, it is more convenient to use trapped atoms such as quantum dots. Quantum dots have a nano-second lifetime and could in principle create gigahertz-rate single photon streams. Almost perfect purity and indistinguishability can be obtained by self-assembled quantum dots in cavities [31]. In order to integrate the single photon source in a quantum network it needs to be coupled efficiently to a single-mode optical fiber.

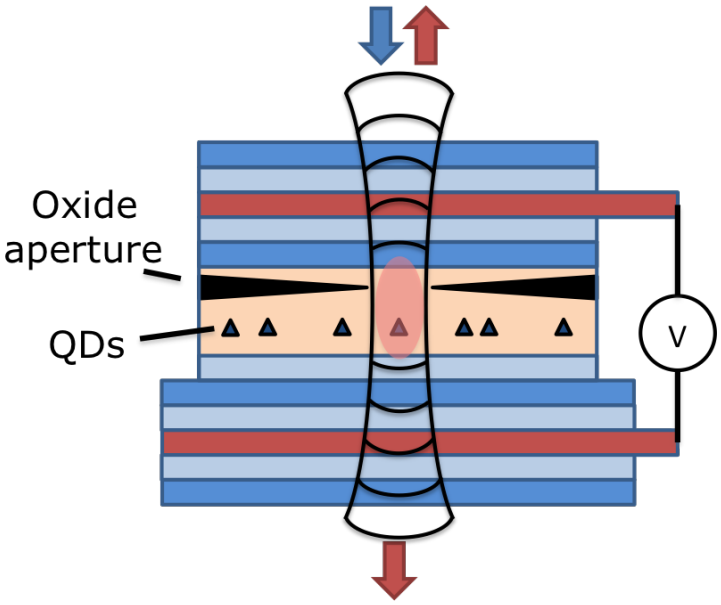

Figure 3.5: *Schematic cross-section of a micropillar cavity. Figure adapted from [32].*

The single-photon source at our disposal consists of a layer of self assembled InAs/GaAs QDs embedded in a micropillar Fabry-Perot cavity. To enable tuning of the QD resonance frequency, which lies around 930 nm, via the quantum confined Stark effect, the QD layer is placed between a p- and an n-contact so that a p-i-n junction is formed. Single mode fibers are attached to the front and the back of the cavity, see figure 3.5.

The purity of the source is verified by a $g^{(2)}(\tau)$ measurement taken with a pulsed laser with a 20 ps pulse length and 12.5 ns period. As the jitter of the single photon detectors is no longer a limiting factor, this gives a more accurate value of $g^{(2)}(0)$ than use of a continuous wave laser. The measured value of $g^{(2)}(0) = 0.037 \pm 0.012$ is most likely limited by the excitation laser which is not perfectly extinguished. In figure 3.6 the second order correlation $g^{(2)}(0)$ is measured as function of excitation power of a continuous wave laser. The strong deviation from 0 occurs due to non-perfect extinction of the laser light. The single photon rate is measured simultaneously, showing rates up to almost 100 MHz.

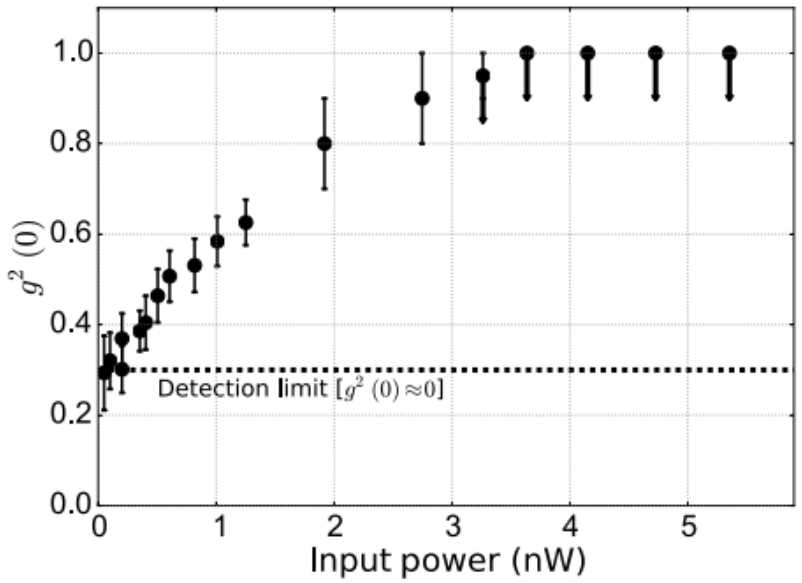

(a)

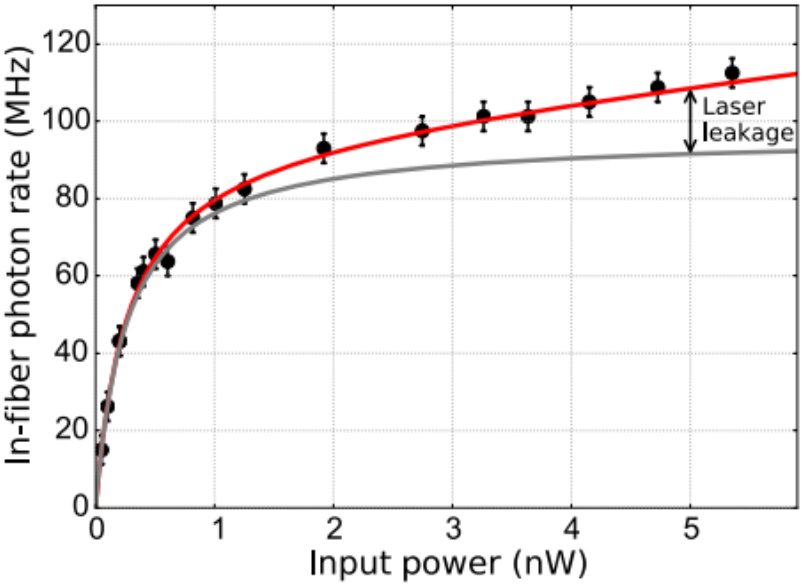

(b)

Figure 3.6: *Simultaneous $g^{(2)}(0)$ and single photon rate measurements dependent on the incident laser power under continuous wave excitation. (a) The detector jitter sets a limit on $g(2)$ which is indicated by the dashed line. The nonperfect extinction of the laser results in a deviation from 0 for high input powers. (b) The fit (red line) takes into account the saturation of the QD transition (gray line) and the residual laser light. Images taken with permission from [33].*

Chapter 4

Quantum light spectroscopy

Only a few papers have been published on experiments that actually perform spectroscopy with quantum light. In this chapter I will review some of them. At first I will discuss one paper that demonstrates sub-shot noise measurements using squeezed light. Thereafter, I will show two papers that investigate the influence of the statistics of the excitation light, before finally discussing the only two papers (up to the date of writing) where single photons are used to perform spectroscopy.

4.1 Spectroscopy with squeezed light

In 1983 Walls published a review of the applications of squeezed light to tackle the limit imposed by vacuum fluctuations [34]. Improvements in measurement precision beyond this shot-noise limit have been demonstrated for interferometry purposes [35, 36] and for the detection of directly encoded amplitude modulation [37]. Spectroscopy measurements are more complicated because the squeezed light source needs to be tunable in frequency.

Polzik et al. demonstrated in 1992 an enhanced sensitivity in saturation spectroscopy measurements of Doppler-free resonances of atomic cesium [38]. In their experiments the squeezed light is generated by an optical parametric oscillator, shown in figure 4.1, and can be tuned by tuning the excitation laser and varying the cavity length. The squeezed part of the light is detected via a balanced homodyne detection scheme. The authors report a reduction of 5.0dB below the vacuum-state level in the photocurrent noise for their frequency tunable squeezed light source and an im-

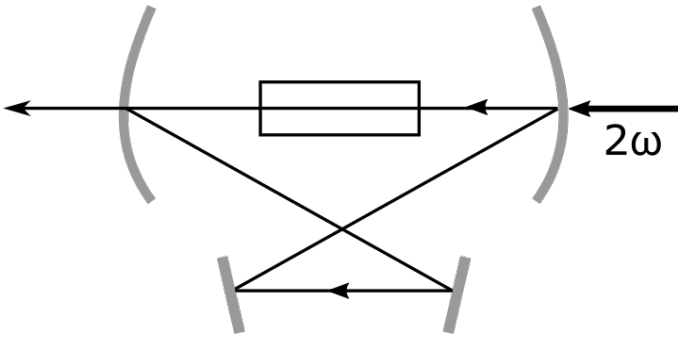

Figure 4.1: *Optical parametric oscillator used to generate the squeezed field.*

provement of 3.1dB for the detection of Doppler-free resonances in atomic cesium.

At this point it should be mentioned that the use of squeezed light not only influences the measurement precision, but also effects the atom-field interaction which can lead to changes in fundamental atomic radiative processes. This has been explored already theoretically following the work of Gardiner [39].

4.2 The influence of statistics of the excitation source on the emission statistics

Usually, the temporal and spectral properties of light fields are considered the most important in optical spectroscopy, but the quantum statistics of light fields matter as well. A way to investigate its influence is photon-statistics excitation spectroscopy. In the following papers the influence of excitation statistics is further investigated for coherent and pseudo-chaotic light sources on a micropillar laser and on a two level system. As a pseudo-thermal light source a Martienssen lamp [40] is used, where a laser is focused on a rotating ground glass disk. The reflection on multiple moving scatterers broadens the spectrum and introduces chaotic intensity fluctuations. The thermal statistics were confirmed by measuring a second order correlation function of approximately 2.

The paper by Kazimierczuk et al. [41] explores the idea that the response of a system to excitation with light of arbitrary quantum statistics can be expressed using the response to coherent states. They demonstrate this for the photon statistics of the emission from a micropillar.

In the basis of coherent states a single thermal mode can be written

as a normal distribution, which results in the known photon number distribution for thermal light. The response of a system could in principle be determined by the weighted response of Fock states. However, Fock states with large photon numbers ($10^6 - 10^7$) are not accessible. Because of these large photon numbers, it is sufficient to measure a coarse grained probability distribution, by binning photon numbers, instead of measuring the full distribution. For a reasonable bin size a coherent state is almost indistinguishable from a Fock state with the same mean photon number. Thus in theory the response to thermal light can be calculated as a weighted sum of responses to coherent inputs.

The input/output curves as a function of mean photon number of a micropillar laser are measured for excitation with both a coherent laser and with a pseudo thermal source. The curves differ in threshold where nonlinear behaviour starts. To test the theory that this difference arises due to the photon statistics, the expected thermal response is calculated from the coherent response. Taking into account saturation levels, the curves show significant overlap. These results suggest that the properties derived from the input/output curve alone is not sufficient to characterize a laser and that the statistics of the pump source need to be taken into account.

The paper by Strauß et al. [42] describes the influence of photon statistics on the excitation dynamics of a single two-level system (TLS) for which self assembled InGaAs quantum dots are used. Two prominent features of TLS interacting with a coherent field are the Mollow triplet and Rabi oscillations. The Mollow triplet can be explained by the dressed states. However, since this picture only holds in the limit where the mean photon number is much higher than the variance, the satellite peaks should disappear in the case of chaotic light where these are approximately equal. Furthermore it has theoretically been predicted that the Rabi oscillations should be repressed by the fluctuations of a chaotic field. It is experimentally observed that both features are indeed absent in the case of pseudo-thermal excitation. These results shows that depending on the photon statistics of the exciting light the response of a TLS differs significantly. Finally, it is shown by a second order correlation measurement of the emitted radiation that the nonclassical nature is preserved as indicated by a dip below zero for $g^{(2)}(0)$.

4.3 Single photon spectroscopy

The excitation statistics do matter, as explained by the examples above. However, both these cases are examples in the regime of high photon numbers. For very low photon numbers the effect has not been explored. As pointed out earlier, the single photons are the purest form of squeezed light. They have the additional advantage that there does not need to be a homodyne detection scheme involved to measure them. The key problems of single photon spectroscopy are the tunability of the source, the difficulty of achieving efficient emitter-photon interfacing and the detection on top of a background.

Only two papers have been published about experiments that perform spectroscopy with single photons. In both experiments, the single photon source is the organic dye molecule dibenzanthantrene (DBATT) in an organic matrix that is placed in a cryostat at 1.4 K. The DBATT molecule is excited via a 01 transition to the first excited vibrational state by illumination of a dye laser. The 00 spontaneous emission between vibrational ground states can be tuned by means of a Stark voltage and is filtered from the laser light by a dichroic mirror. The inhomogeneity of the 00 zero phonon lines frequencies ensures that individual molecules can be excited selectively.

The most recent paper, by Kiefer et al. [43], does not go into detail about the properties of the single photons. The goal is to demonstrate that the atomic spectrum of a Faraday anomalous dispersion optical filter can be recorded with a single molecule as single photon source.

The most relevant work for this project was published in 2012 by Rezus et al. [44] on single photon spectroscopy of a single molecule. In their experiments, a second DBATT molecule under the same conditions as the source molecule was excited with the narrowband 00 emission of the source molecule. The extinction of this light beam was examined as function of the detuning frequency. A simplified version of their setup is shown in figure 4.2. The source molecule was reported to produce single photons at a rate of $4 \cdot 10^5$ s^{-1}.

The extinction of a light beam can be described by considering the incident and scattered fields [45]. A simulation of the probability amplitudes with parameters obtained from the scanning of the target molecule with a tunable laser agreed very well with the experimental data.

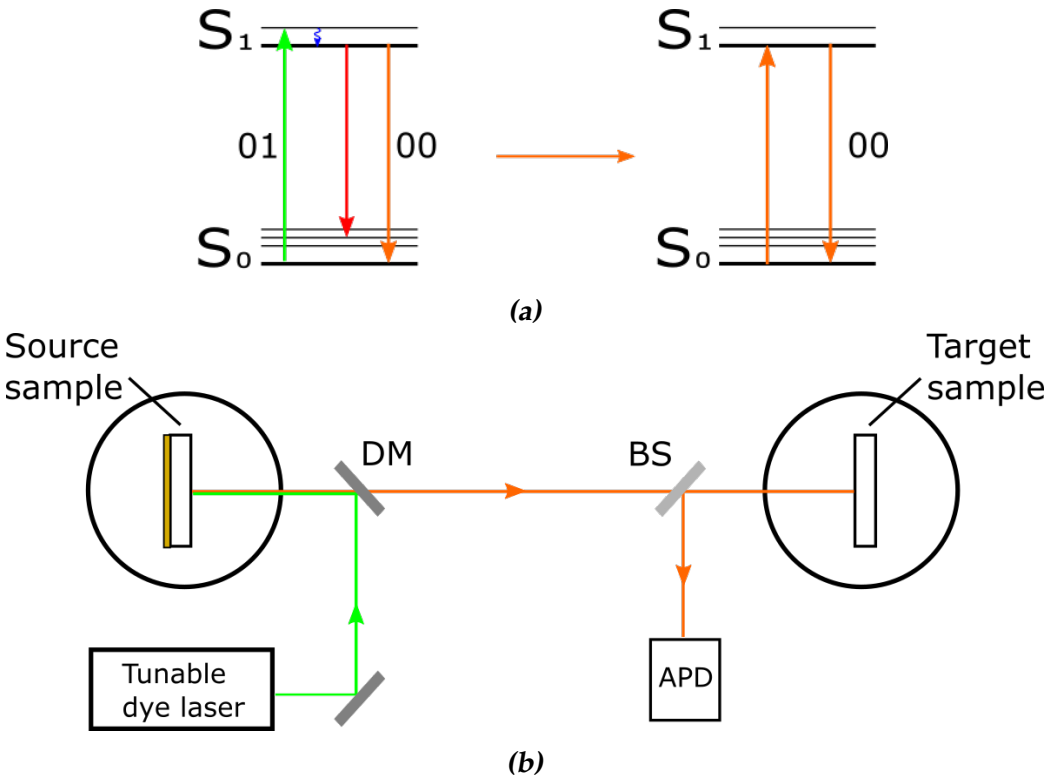

Figure 4.2: *(a) Molecular excitation scheme. (b) Illustration of a simplified version of the single photon microscopy setup. The source and target samples are inside a cryogenic microscopes at 1.4K. Microelectrodes are connected to the source sample. DM, dichroic mirror; BS, 50:50 beam splitter; APD, avalanche photodiode. Figure adapted from [44].*

One of the problems that the authors tackled is the creation of a tunable single photon source in order to do spectroscopy. They tuned the frequency of the fluorescence photons of the source molecule via the Stark effect. The next challenge is the detection of the weak photon stream on top of a background. For dipole allowed transitions the typical fluorescence lifetime is of the order of 0.1 to 10 ns, which corresponds to a radiated power of 0.03 to 3 nW. Although most of the fluorescence can be collected using dielectric antennas [46], the usable power is further limited by losses in the detection path. If the detection efficiency is large enough, it should in principle be possible to measure the fluorescence instead of an extinction spectrum.

Chapter 5

Conclusion

In biomicroscopy fluorescence is used to image living tissue. Most conventional organic fluorophores emit in the visual range. They have a small Stokes shift and narrow absorption and emission spectra. Quantum dots can be used as fluorescent markers as well. They have the advantage that they can be excited at any wavelength below their characteristic absorption wavelength. This enables color labeling while using one excitation source. Additionally, quantum dots can be tuned by their diameter to emit near infrared wavelengths, which has the benefits that it penetrates deeper into a sample and is less prone to scattering effects. There is, however, a caveat. Water absorbs more at higher wavelengths and this introduces additional losses. An important limiting factor in fluorescence measurements is that after some time all emitters are bleached. Photobleaching processes involve transitions to reactive triplet or anion states and reactions with radical oxygen. Quantum dots are generally less affected by photobleaching than organic fluorophores and have been shown to be photostable for hours.

The goal of this thesis was to gain insight whether single photon excitation in biomicroscopy is feasible and if this would solve the problem of photobleaching. Since multiphoton processes are heavily repressed when exciting with single photons, I expect that the chance for a molecule to end up in a multiple excited state is lower than for coherent excitation. Since these states are highly reactive and play a role in photobleaching, I expect that as a result the bleaching rate reduces as well. The generation of radical oxygen will then also be repressed, which in turn also decreases the cytotoxicity. Furthermore, the use of squeezed light, in particular single photons, allows sub-shot noise measurements. This is of great interest

when working with samples that have weak optical responses that would generally not be distinguishable from the noise. One of the difficulties of working with squeezed light is that any form of loss will degrade the statistics back to the Poissonian case. Another limitation in the case of single photons is that the sources are not very bright, often with powers of the order of 10^{-15} W compared to coherent light sources that can easily generate streams of the order of 10^{-3} W. It is therefore challenging to obtain a significant signal-to-noise ratio. Nevertheless, it has been shown that spectroscopy can be performed with single photons when measuring an extinction spectrum. Time resolved measurements, however, such as tracking of proteins, are currently impossible to do with single photons.

So far, single photon experiments have only been done with single photon sources without cavities. By placing a single photon source in a cavity, it is possible to enhance the rate to the GHz regime [47]. This will enable new types of measurements. The single photon source at our disposal already looks promising to start experiments. After some search I found a PbS based quantum dot with an absorption spectrum that is compatible with the 930 nm emission of the source (shown in figure 2.9). After integrating the single photons in the microscopy setup, this can be the first test system for single photon microscopy with a bright single photon source.

Bibliography

[1] C. Antón, J. C. Loredo, G. Coppola, H. Ollivier, N. Viggianiello, A. Harouri, N. Somaschi, A. Crespi, I. Sagnes, A. Lemaître, L. Lanco, R. Osellame, F. Sciarrino, and P. Senellart, *Interfacing scalable photonic platforms: solid-state based multi-photon interference in a reconfigurable glass chip*, (2019).

[2] E. U. Condon, *Nuclear Motions Associated with Electron Transitions in Diatomic Molecules*, Phys. Rev. **32**, 858 (1928).

[3] A. D. McNaught and A. Wilkinson, *IUPAC. Compendium of Chemical Terminology (the "Gold book")*, Blackwell Scientific Publications, Oxford, 2nd edition, 1997.

[4] J. R. Lakowicz, *Principles of fluorescence spectroscopy*, Springer-Verlag, New York, 3rd ed.. edition, 2006.

[5] S. Adachi, *GaAs, AlAs, and AlxGa1xAs: Material parameters for use in research and device applications*, J. Appl. Phys. **58**, R1 (1985).

[6] C. F. Klingshirn, *Semiconductor optics*, Springer-Verlag, Berlin Heidelberg, 2nd edition, 2005.

[7] T. Numai, *Fundamentals of Semiconductor Lasers*, Springer-Verlag, New York, 2004.

[8] A. P. Alivisatos, *Semiconductor Clusters, Nanocrystals, and Quantum Dots*, Science (80-.). **271**, 933 (1996).

[9] S. Baskoutas and A. F. Terzis, *Size-dependent band gap of colloidal quantum dots*, J. Appl. Phys. **99**, 013708 (2006).

[10] D. Vasudevan, R. R. Gaddam, A. Trinchi, and I. Cole, *Core–shell quantum dots: Properties and applications*, J. Alloys Compd. **636**, 395 (2015).

[11] A. S. Karakoti, R. Shukla, R. Shanker, and S. Singh, *Surface functionalization of quantum dots for biological applications*, Adv. Colloid Interface Sci. **215**, 28 (2015).

[12] D. Gerion, F. Pinaud, S. C. Williams, W. J. Parak, D. Zanchet, S. Weiss, and A. P. Alivisatos, *Synthesis and Properties of Biocompatible Water-Soluble Silica-Coated CdSe/ZnS Semiconductor Quantum Dots*, J. Phys. Chem. B **105**, 8861 (2001).

[13] A. M. Derfus, W. C. W. Chan, and S. N. Bhatia, *Probing the Cytotoxicity of Semiconductor Quantum Dots*, Nano Lett. **4**, 11 (2004).

[14] A. Diaspro, G. Chirico, C. Usai, P. Ramoino, and J. Dobrucki, *Photobleaching*, in *Handb. Biol. Confocal Microsc.*, edited by J. B. Pawley, pages 690–702, Springer US, Boston, MA, 2006.

[15] R. Zondervan, F. Kulzer, M. A. Kol'chenk, and M. Orrit, *Photobleaching of Rhodamine 6G in Poly(vinyl alcohol) at the Ensemble and Single-Molecule Levels*, J. Phys. Chem. A **108**, 1657 (2004).

[16] M. Nirmal, B. O. Dabbousi, M. G. Bawendi, J. J. Macklin, J. K. Trautman, T. D. Harris, and L. E. Brus, *Fluorescence intermittency in single cadmium selenide nanocrystals*, Nature **383**, 802 (1996).

[17] H. Qin, R. Meng, N. Wang, and X. Peng, *Photoluminescence Intermittency and Photo-Bleaching of Single Colloidal Quantum Dot*, Adv. Mater. **29**, 1606923 (2017).

[18] W. G. J. H. M. van Sark, P. L. T. M. Frederix, D. J. Van den Heuvel, H. C. Gerritsen, A. A. Bol, J. N. J. van Lingen, C. de Mello Donegá, and A. Meijerink, *Photooxidation and Photobleaching of Single CdSe/ZnS Quantum Dots Probed by Room-Temperature Time-Resolved Spectroscopy*, J. Phys. Chem. B **105**, 8281 (2001).

[19] S.-J. Yu, M.-W. Kang, H.-C. Chang, K.-M. Chen, and Y.-C. Yu, *Bright Fluorescent Nanodiamonds: No Photobleaching and Low Cytotoxicity*, J. Am. Chem. Soc. **127**, 17604 (2005).

[20] I. R. Berchera and I. P. Degiovanni, *Quantum imaging with sub-Poissonian light: challenges and perspectives in optical metrology*, Metrologia **56**, 024001 (2019).

[21] M. Fox, *Quantum Optics: An Introduction*, Oxford University Press, 2006.

[22] I. A. Walmsley, *Quantum optics: Science and technology in a new light*, Science (80-.). **348**, 525 (2015).

[23] A. I. Lvovsky, *Squeezed light*, (2014).

[24] K. E. Dorfman, F. Schlawin, and S. Mukamel, *Nonlinear optical signals and spectroscopy with quantum light*, Rev. Mod. Phys. **88**, 45008 (2016).

[25] D. C. Burnham and D. L. Weinberg, *Observation of Simultaneity in Parametric Production of Optical Photon Pairs*, Phys. Rev. Lett. **25**, 84 (1970).

[26] S. P. Walborn, C. H. Monken, S. Pádua, and P. H. Souto Ribeiro, *Spatial correlations in parametric down-conversion*, Phys. Rep. **495**, 87 (2010).

[27] B. Lounis and M. Orrit, *Single-photon sources*, Reports Prog. Phys. **68**, 1129 (2005).

[28] C. Gardiner and C. Savage, *A multimode quantum theory of a degenerate parametric amplifier in a cavity*, Opt. Commun. **50**, 173 (1984).

[29] J. Javanainen and P. L. Gould, *Linear intensity dependence of a two-photon transition rate*, Phys. Rev. A **41**, 5088 (1990).

[30] M. D. Eisaman, J. Fan, A. Migdall, and S. V. Polyakov, *Invited Review Article: Single-photon sources and detectors*, Rev. Sci. Instrum. **82**, 071101 (2011).

[31] N. Somaschi, V. Giesz, L. De Santis, J. C. Loredo, M. P. Almeida, G. Hornecker, S. L. Portalupi, T. Grange, C. Antón, J. Demory, C. Gómez, I. Sagnes, N. D. Lanzillotti-Kimura, A. Lemaítre, A. Auffeves, A. G. White, L. Lanco, and P. Senellart, *Near-optimal single-photon sources in the solid state*, Nat. Photonics **10**, 340 (2016).

[32] H. J. Snijders, *Quantum Dot Microcavity Control of Photon Statistics*, PhD thesis, Leiden University, 2018.

[33] H. Snijders, J. Frey, J. Norman, V. Post, A. Gossard, J. Bowers, M. van Exter, W. Löffler, and D. Bouwmeester, *Fiber-Coupled Cavity-QED Source of Identical Single Photons*, Phys. Rev. Appl. **9**, 31002 (2018).

[34] D. F. Walls, *Squeezed states of light*, Nature **306**, 141 (1983).

[35] P. Grangier, R. E. Slusher, B. Yurke, and A. LaPorta, *Squeezed-light–enhanced polarization interferometer*, Phys. Rev. Lett. **59**, 2153 (1987).

[36] M. Xiao, L.-A. Wu, and H. J. Kimble, *Precision measurement beyond the shot-noise limit*, Phys. Rev. Lett. **59**, 278 (1987).

[37] M. Xiao, L.-A. Wu, and H. J. Kimble, *Detection of amplitude modulation with squeezed light for sensitivity beyond the shot-noise limit*, Opt. Lett. **13**, 476 (1988).

[38] E. S. Polzik, J. Carri, and H. J. Kimble, *Spectroscopy with squeezed light*, Phys. Rev. Lett. **68**, 3020 (1992).

[39] C. W. Gardiner, *Inhibition of Atomic Phase Decays by Squeezed Light: A Direct Effect of Squeezing*, Phys. Rev. Lett. **56**, 1917 (1986).

[40] W. Martienssen and E. Spiller, *Coherence and Fluctuations in Light Beams*, Am. J. Phys. **32**, 919 (1964).

[41] T. Kazimierczuk, J. Schmutzler, M. Aßmann, C. Schneider, M. Kamp, S. Höfling, and M. Bayer, *Photon-Statistics Excitation Spectroscopy of a Quantum-Dot Micropillar Laser*, Phys. Rev. Lett. **115**, 27401 (2015).

[42] M. Strauß, M. Placke, S. Kreinberg, C. Schneider, M. Kamp, S. Höfling, J. Wolters, and S. Reitzenstein, *Photon-statistics excitation spectroscopy of a single two-level system*, Phys. Rev. B **93**, 241306 (2016).

[43] W. Kiefer, M. Rezai, J. Wrachtrup, and I. Gerhardt, *An atomic spectrum recorded with a single-molecule light source*, Appl. Phys. B **122**, 38 (2016).

[44] Y. L. A. Rezus, S. G. Walt, R. Lettow, A. Renn, G. Zumofen, S. Götzinger, and V. Sandoghdar, *Single-Photon Spectroscopy of a Single Molecule*, Phys. Rev. Lett. **108**, 93601 (2012).

[45] G. Wrigge, I. Gerhardt, J. Hwang, G. Zumofen, and V. Sandoghdar, *Efficient coupling of photons to a single molecule and the observation of its resonance fluorescence*, Nat. Phys. **4**, 60 (2007).

[46] K. G. Lee, X. W. Chen, H. Eghlidi, P. Kukura, R. Lettow, A. Renn, V. Sandoghdar, and S. Götzinger, *A planar dielectric antenna for directional single-photon emission and near-unity collection efficiency*, Nat. Photonics **5**, 166 (2011).

[47] P. Senellart, G. Solomon, and A. White, *High-performance semiconductor quantum-dot single-photon sources*, Nat. Nanotechnol. **12**, 1026 (2017).